Supplemental Figure 1

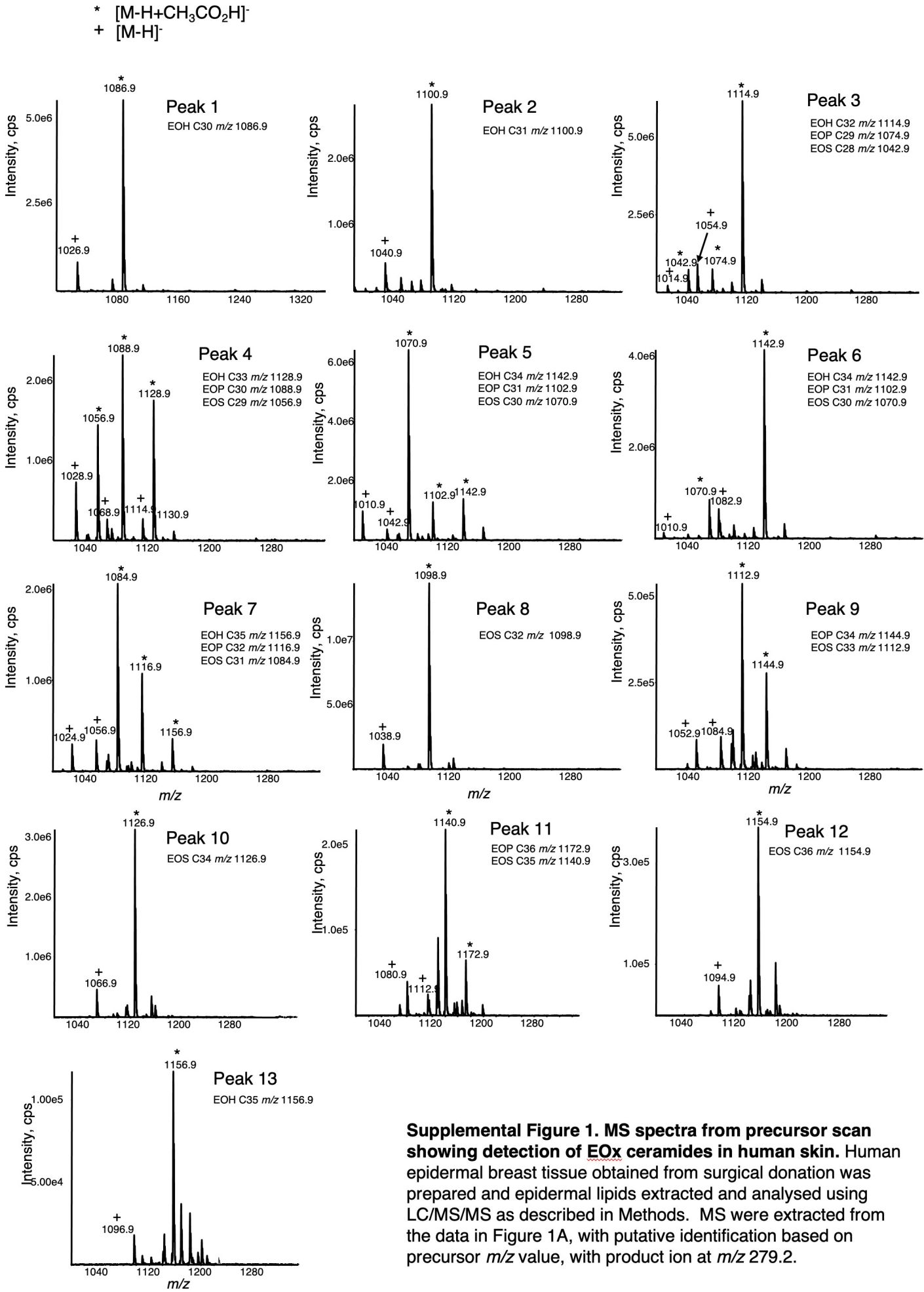

Supplemental Figure 1. MS spectra from precursor scan showing detection of EOx ceramides in human skin. Human epidermal breast tissue obtained from surgical donation was prepared and epidermal lipids extracted and analysed using LC/MS/MS as described in Methods. MS were extracted from the data in Figure 1A, with putative identification based on precursor *m/z* value, with product ion at *m/z* 279.2.

Supplemental Figure 2

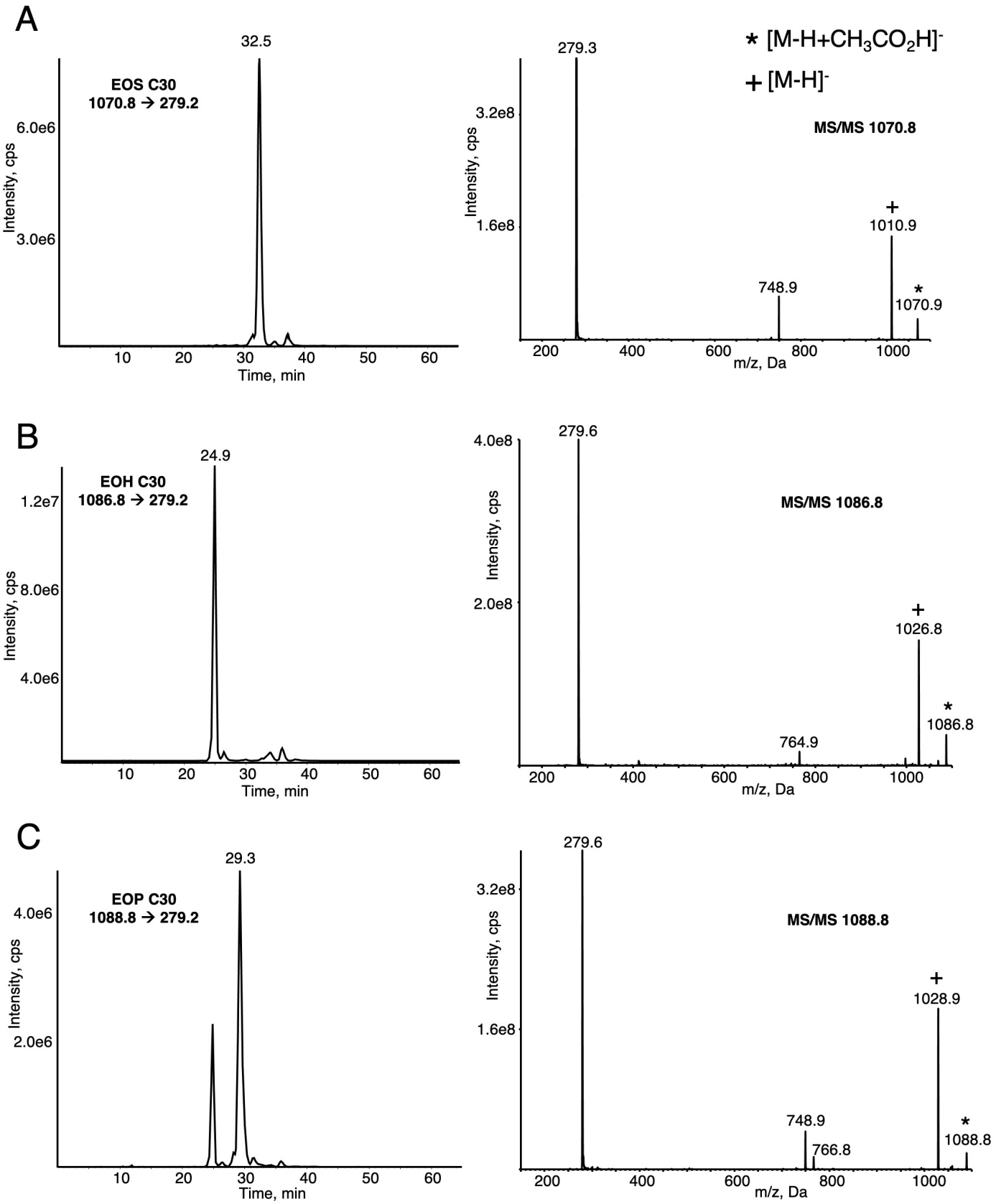

Supplemental Figure 2. MS/MS chromatograms and spectra for LA containing C30-EOx ceramides. Lipids extracted as in Supplemental Figure 1 were analysed using reverse phase LC/MS/MS as described in Methods, monitoring the precursor to product ion as shown in the left panels. Enhanced product ion (EPI) spectra were acquired in ion trap mode at the apex of elution for each lipid as described. Lipids were detected as $[M\text{-}H+CH_3CO_2H]^-$ ions.

Supplemental Figure 3

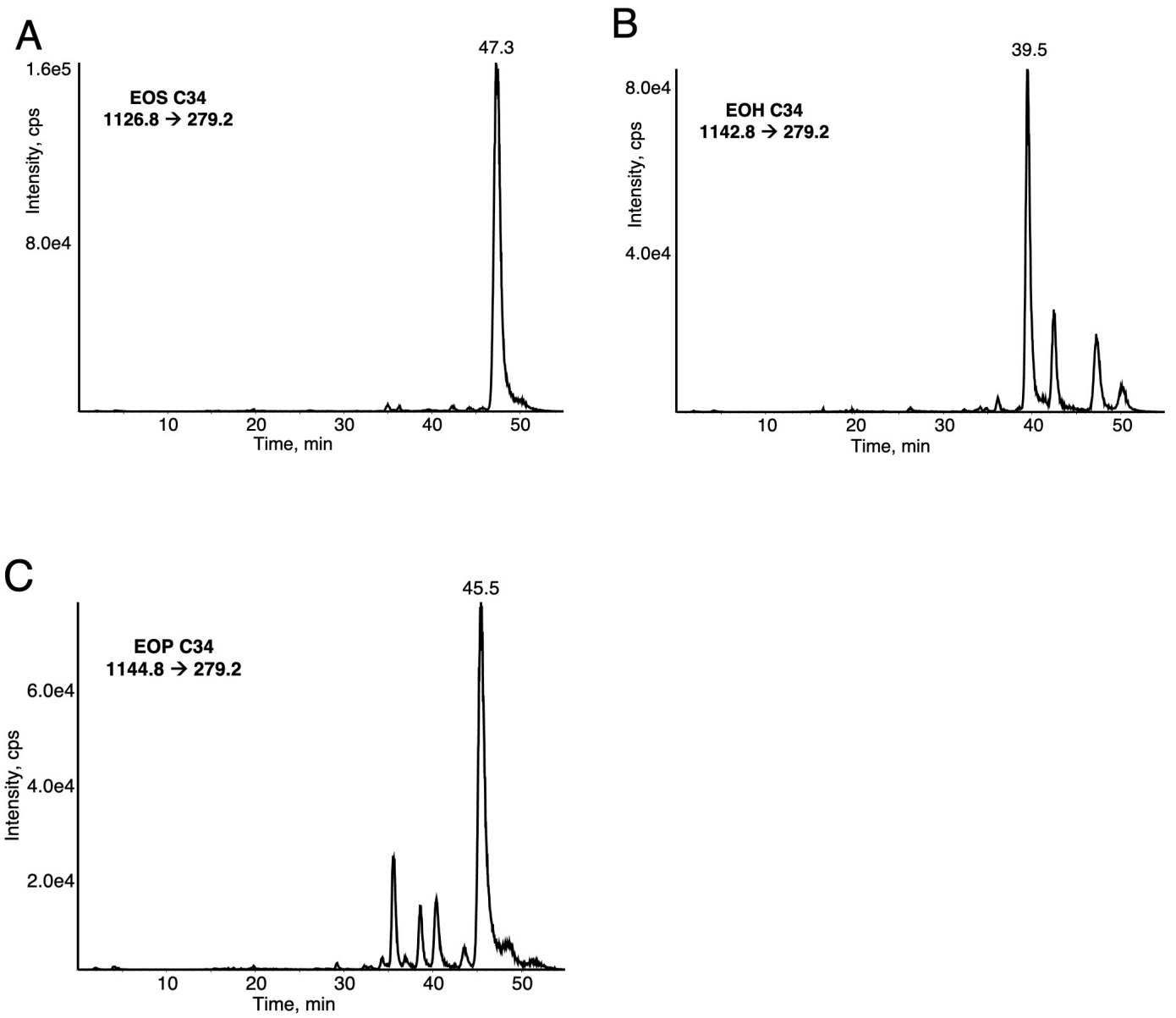

Supplemental Figure 3. MS/MS chromatograms and spectra for LA containing C34-EOx ceramides. Lipids extracted as in Supplemental Figure 1 were analysed using reverse phase LC/MS/MS as described in Methods, monitoring the precursor to product ion as shown in the left panels.

Supplemental Figure 4

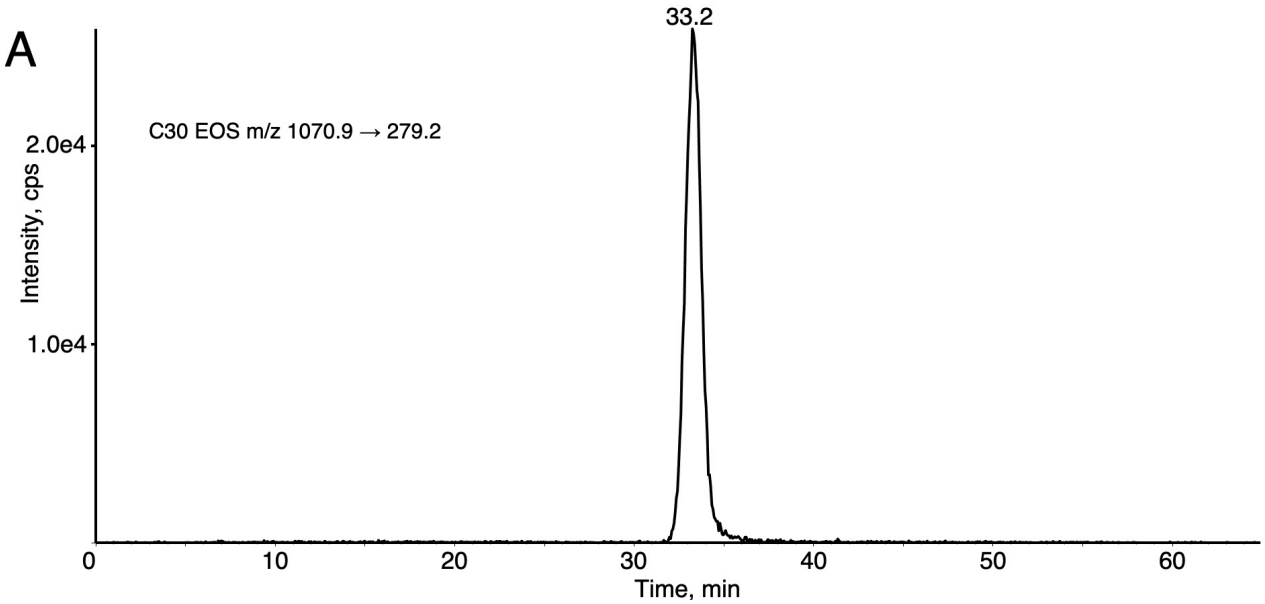

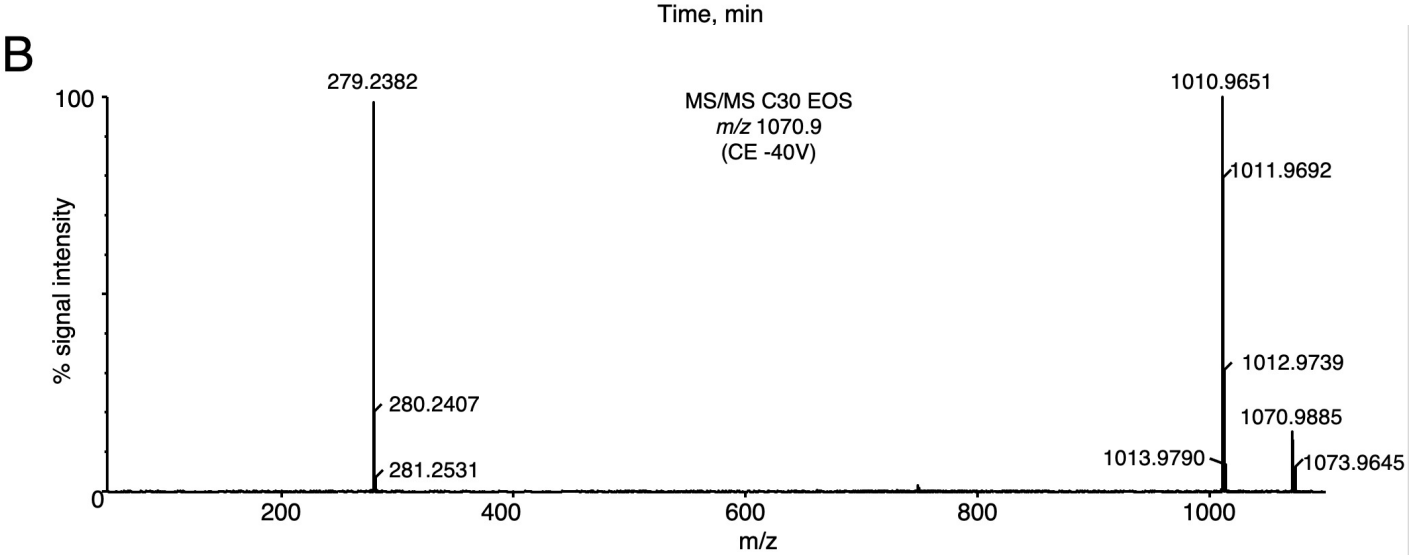

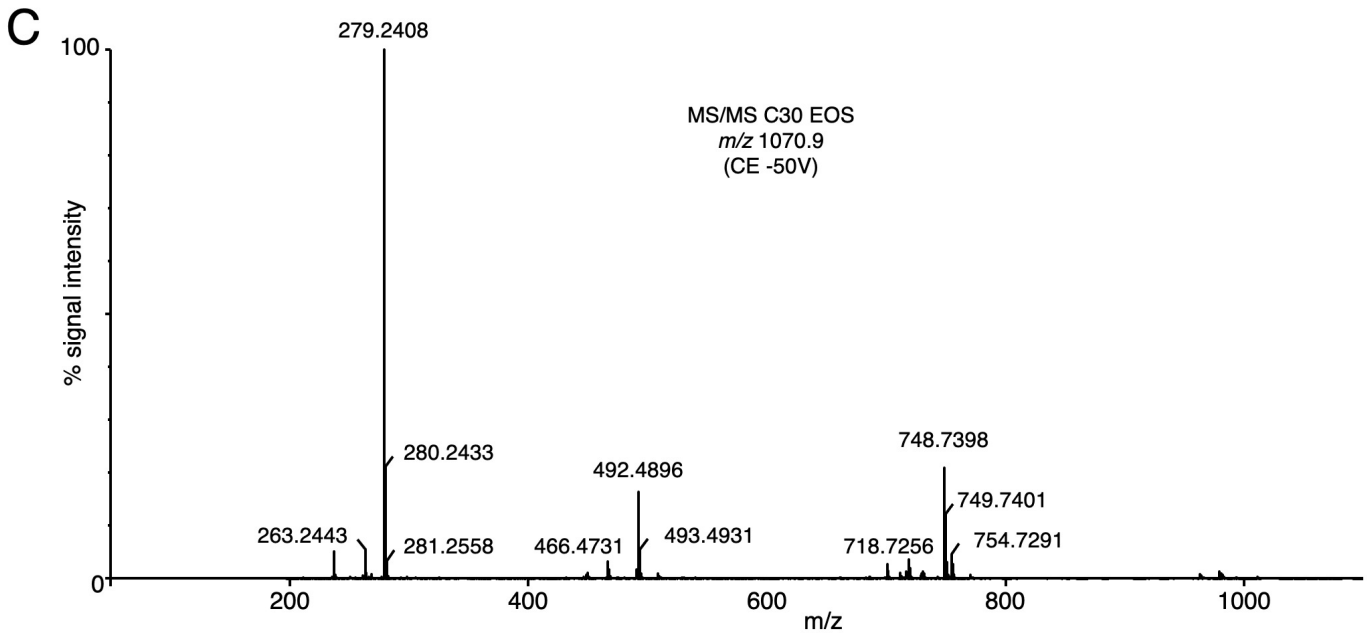

Supplemental Figure 4. C30 EOS standard - confirmation of retention time and high resolution mass spectra. *Panel A* – C30 EOS was analysed using reverse phase LC/MS/MS as described in Methods, monitoring the precursor to product ion as shown. *Panel B, C* - C30-EOS was diluted in 80:20 MeOH: THF + 5mM Ammonium acetate at a concentration of 0.5*µ*g/ml. This was infused at 10*µ*l/min into a Waters Synapt XS QTOF. MS/MS spectra was obtained in high resolution mode with the following settings: capilliary voltage - 2.4kV, sampling cone 35, desolvation temperature 250°C, desolvation gas 350. CE applied was -40V (Panel B) and -50V (Panel C).

Supplemental Figure 5

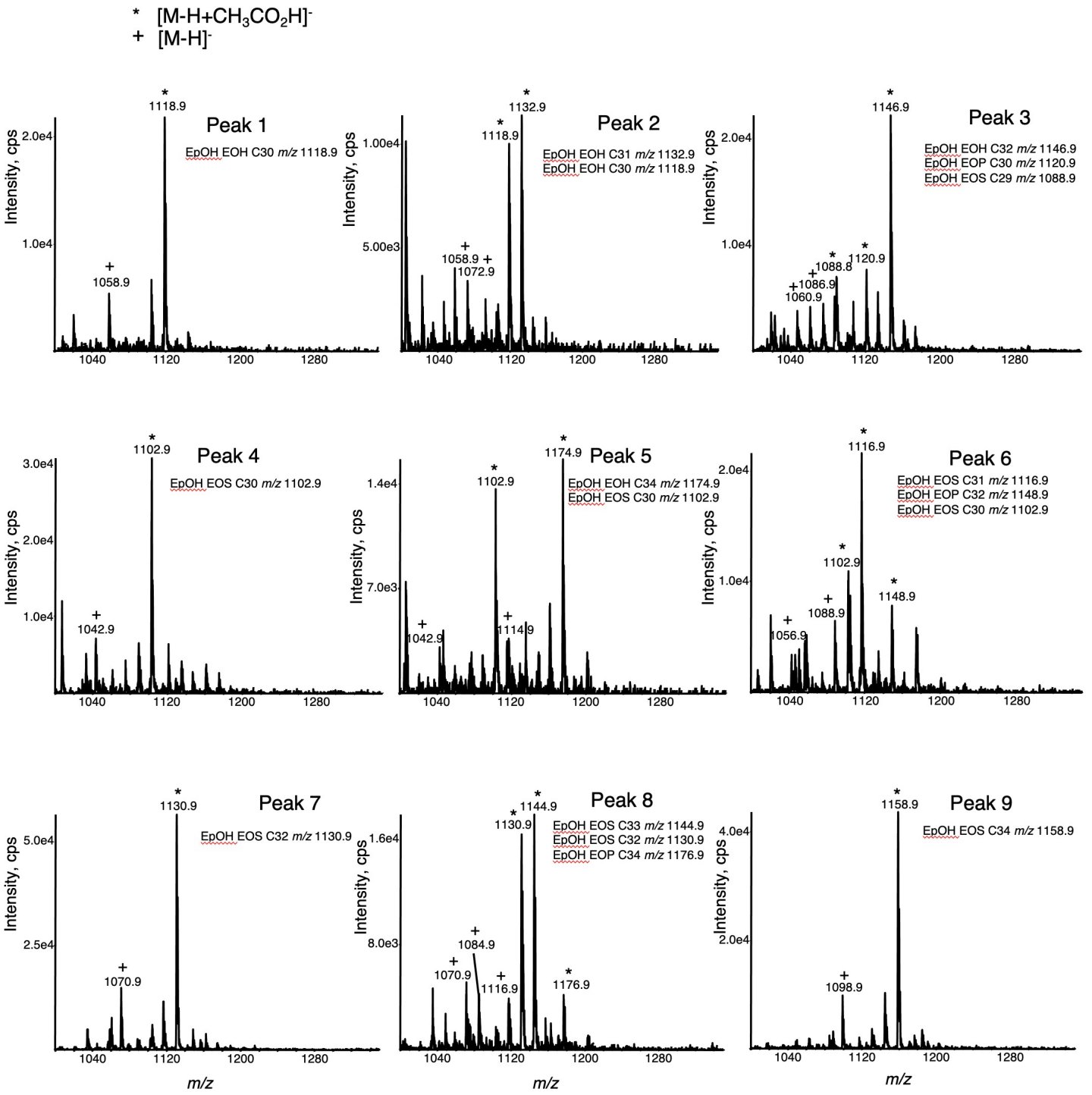

Supplemental Figure 5. MS spectra from precursor scan showing detection of epoxy-HOME EOx ceramides in human skin. Human epidermal breast tissue obtained from surgical donation was prepared and epidermal lipids extracted and analysed using LC/MS/MS as described in Methods. MS were extracted from the data in Figure 1A, with putative identification based on precursor *m/z* value, with product ion at *m/z* 311.2.

Supplemental Figure 6

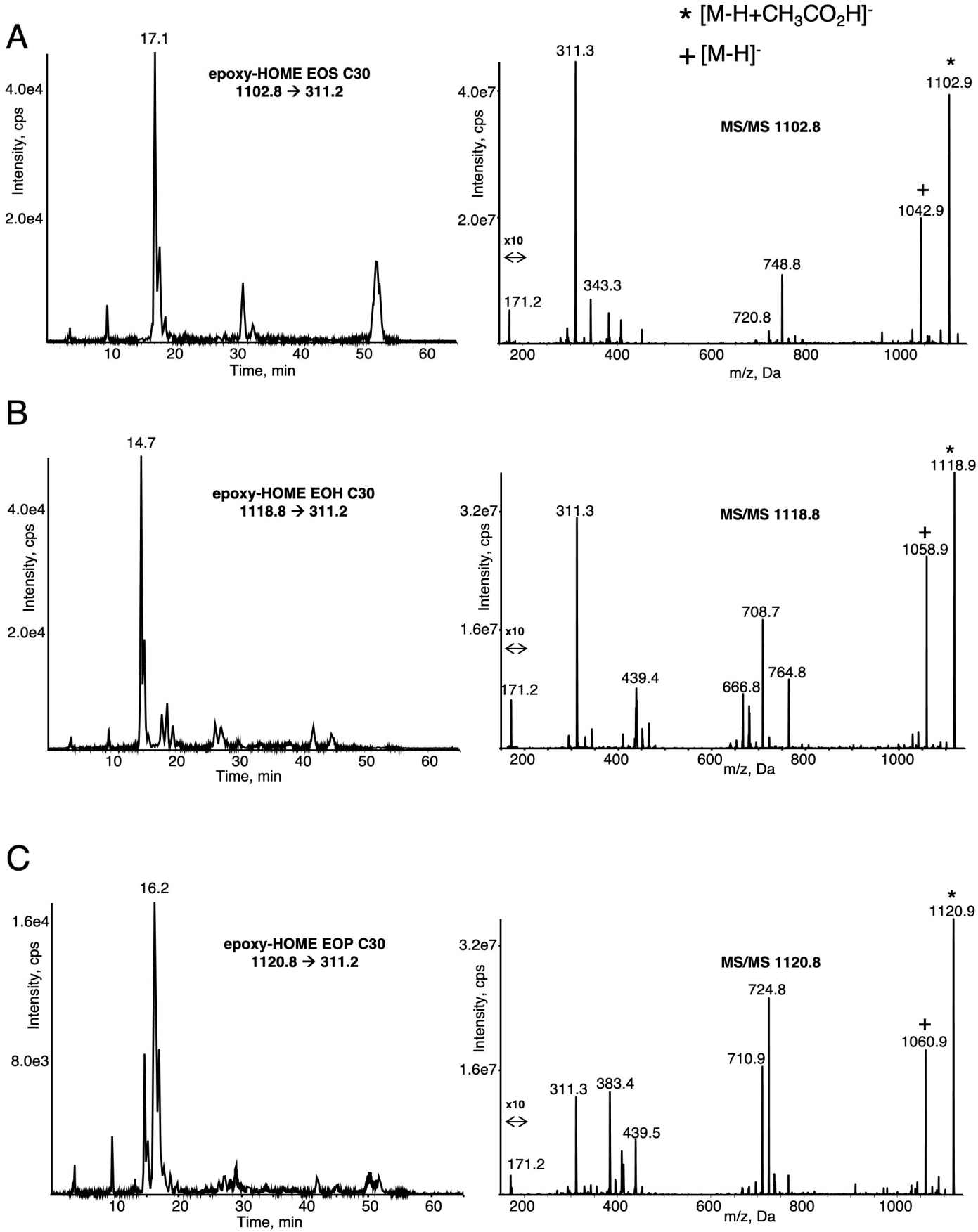

Supplemental Figure 6. MS/MS chromatograms and spectra for epoxy-HOME containing C30-EOx ceramides. Lipids extracted as in Supplemental Figure 5 were analysed using reverse phase LC/MS/MS as described in Methods, monitoring the precursor to product ion as shown in the left panels. Enhanced product ion (EPI) spectra were acquired in ion trap mode at the apex of elution for each lipid as described. Lipids were detected as $[M\text{-}H+CH_3CO_2H]^-$ ions.

Supplemental Figure 7

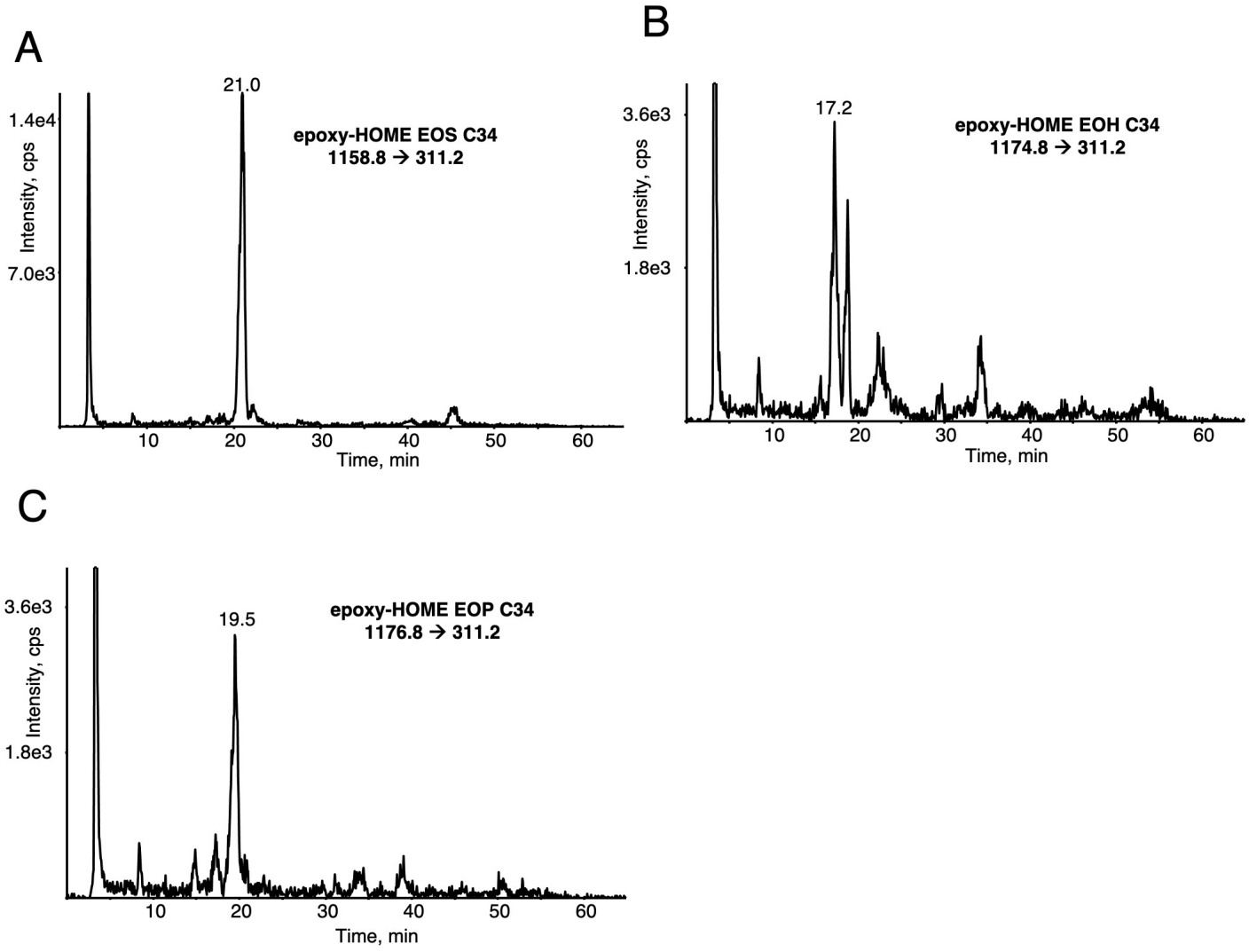

Supplemental Figure 7. MS/MS chromatograms and spectra for epoxy-HOME containing C34-EOx ceramides. Lipids extracted as in Supplemental Figure 5 were analysed using reverse phase LC/MS/MS as described in Methods, monitoring the precursor to product ion as shown in the left panels.

Supplemental Figure 8

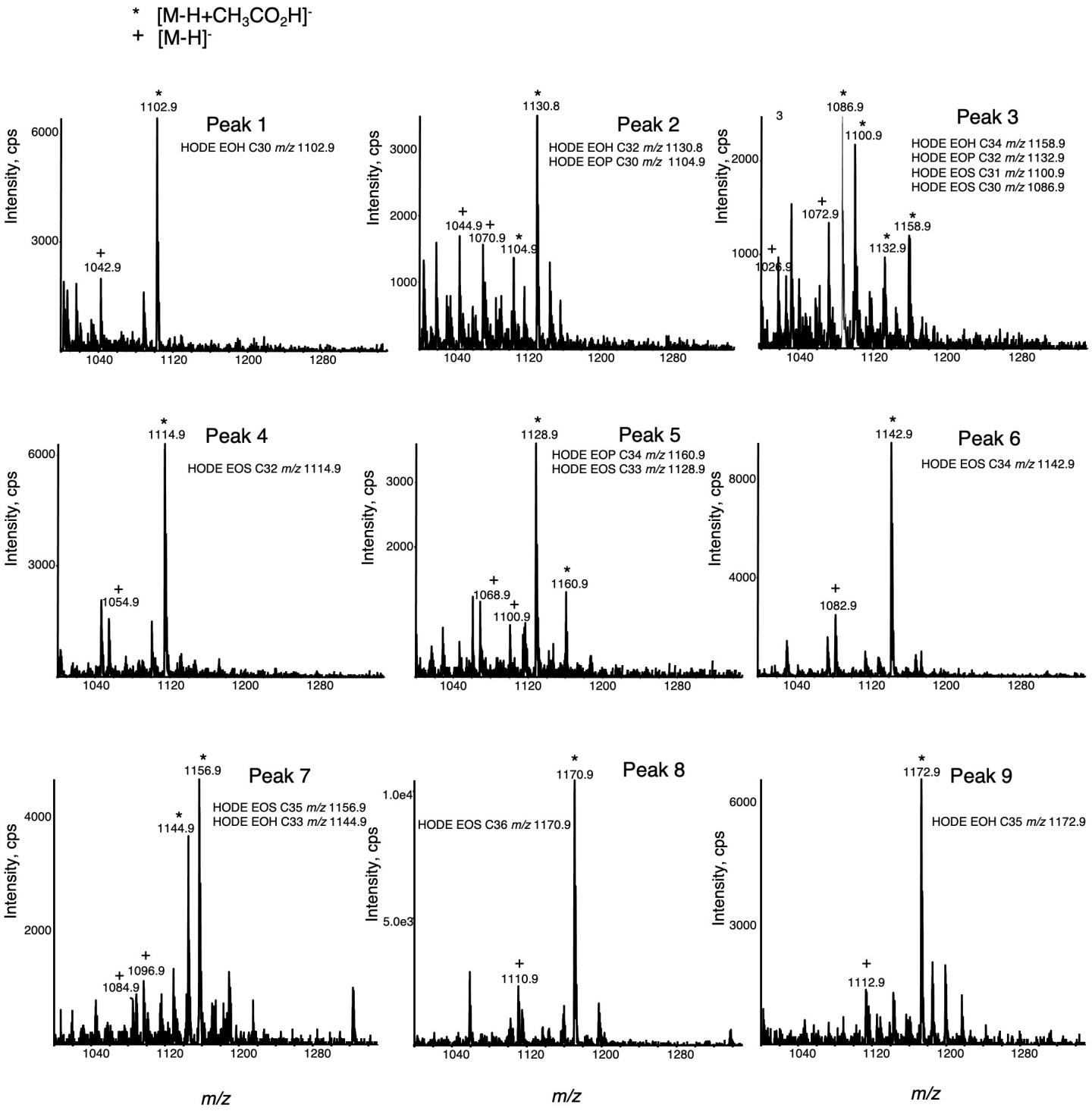

Supplemental Figure 8. MS spectra from precursor scan showing detection of HODE EOx ceramides in human skin. Human epidermal breast tissue obtained from surgical donation was prepared and epidermal lipids extracted and analysed using LC/MS/MS as described in Methods. MS were extracted from the data in Figure 1A, with putative identification based on precursor *m/z* value, with product ion at *m/z* 295.2.

Supplemental Figure 9

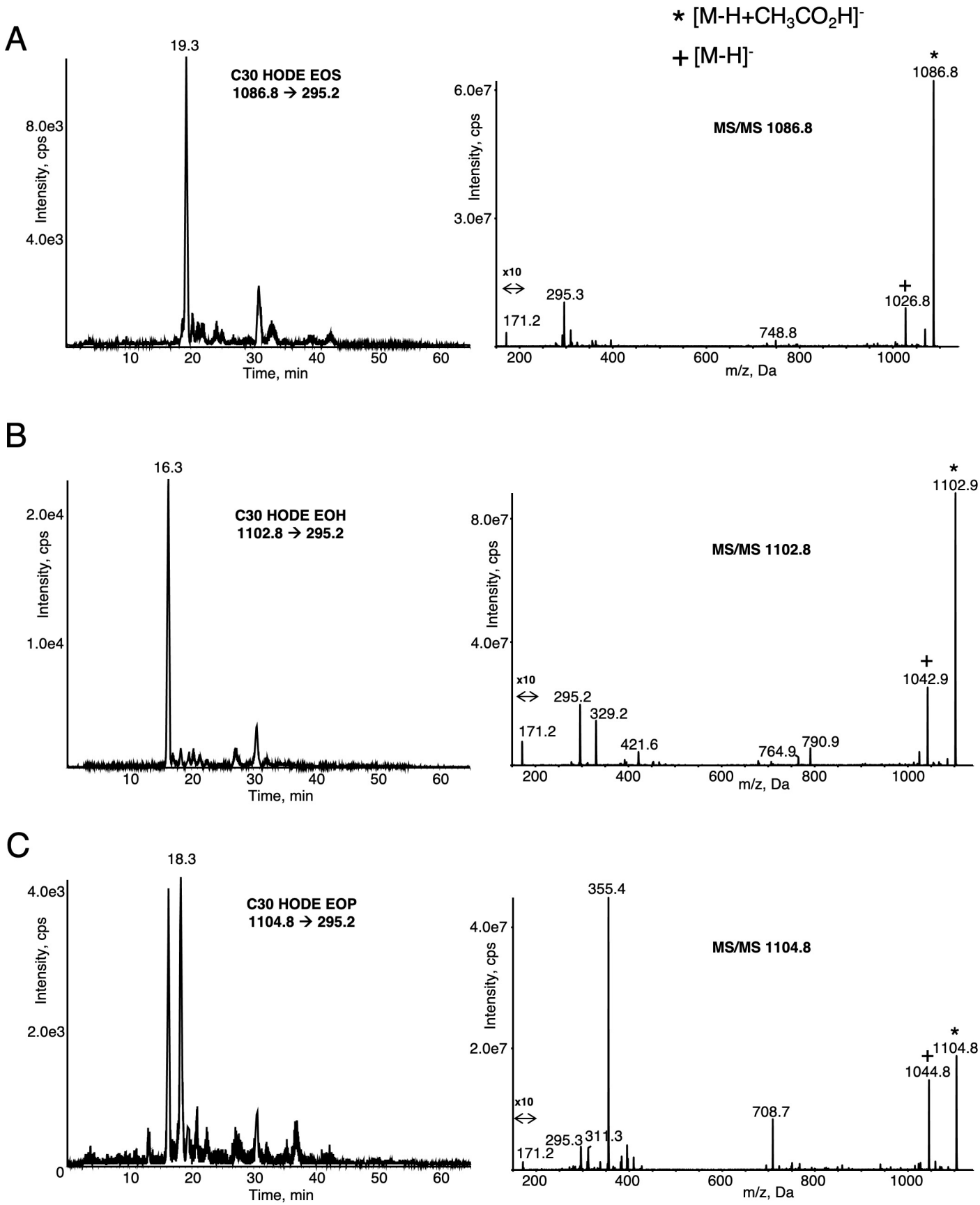

Supplemental Figure 9. MS/MS chromatograms and spectra for HODE containing C30-EOx ceramides. Lipids extracted as in Supplemental Figure 8 were analysed using reverse phase LC/MS/MS as described in Methods, monitoring the precursor to product ion as shown in the left panels. Enhanced product ion (EPI) spectra were acquired in ion trap mode at the apex of elution for each lipid as described. Lipids were detected as [M-H+CH_3CO_2H]$^-$ ions.

Supplemental Figure 10

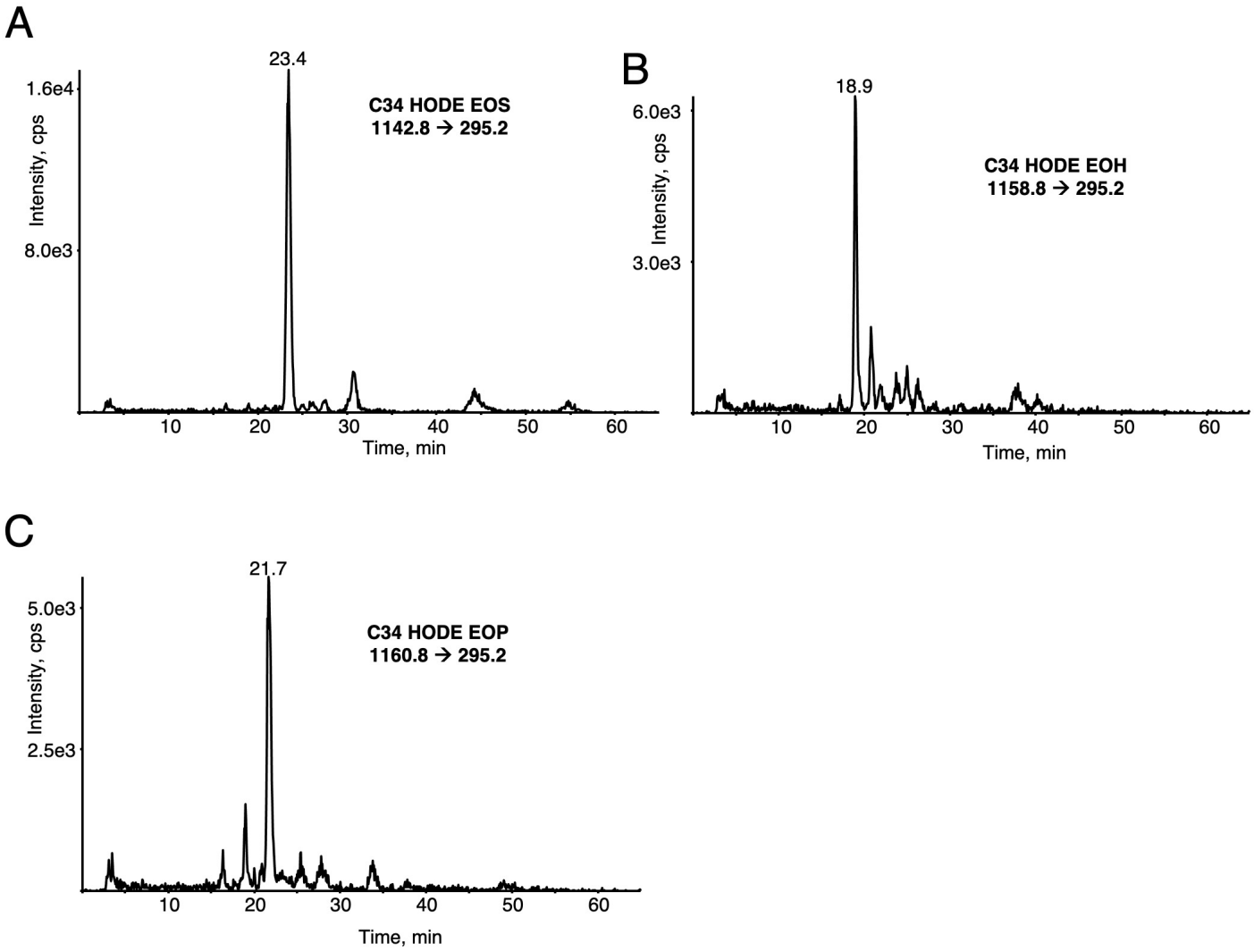

Supplemental Figure 10. MS/MS chromatograms and spectra for HODE containing C34-EOx ceramides. Lipids extracted as in Supplemental Figure 5 were analysed using reverse phase LC/MS/MS as described in Methods, monitoring the precursor to product ion as shown in the left panels.

Supplemental Figure 11

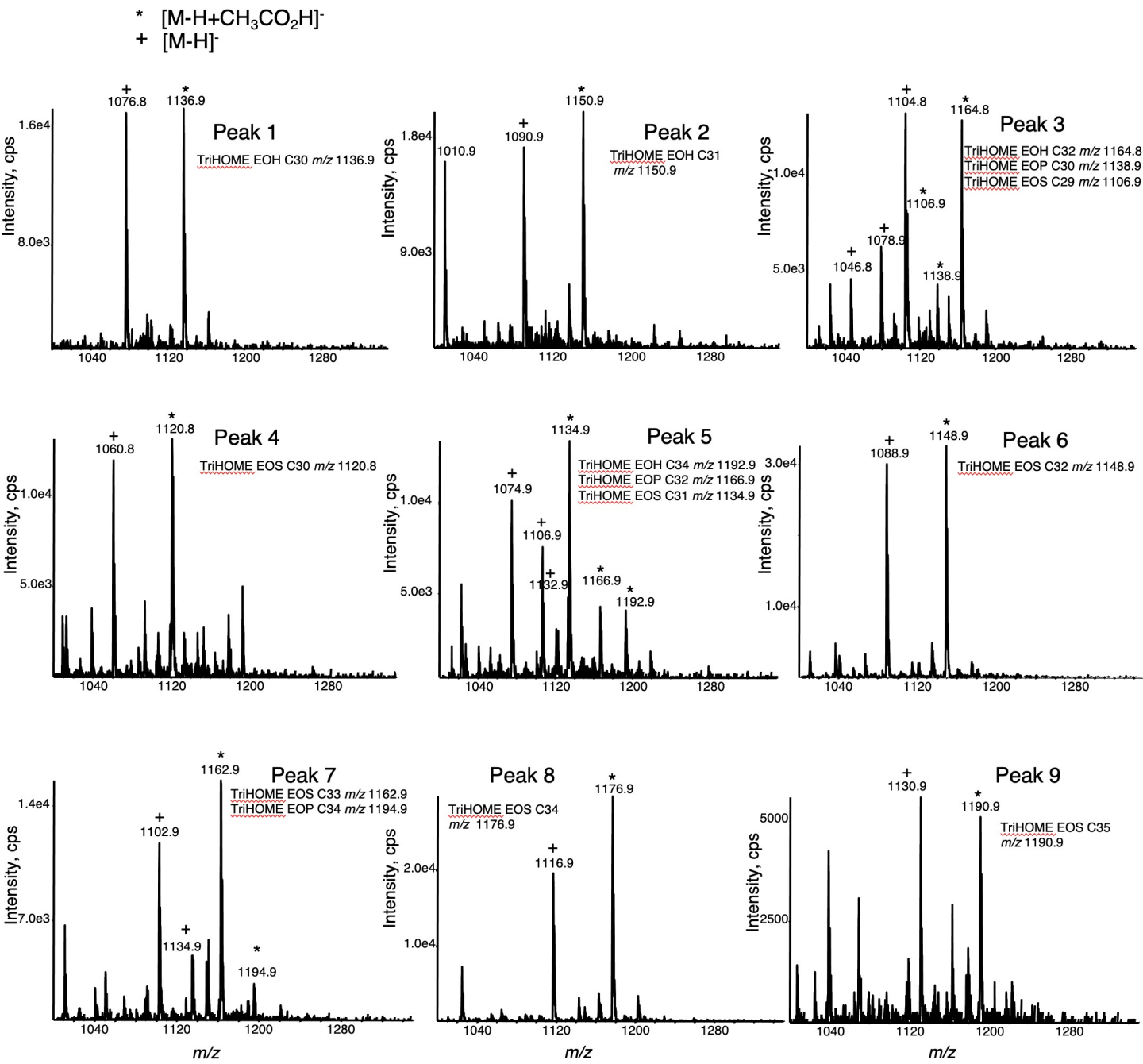

Supplemental Figure 11. MS spectra from precursor scan showing detection of TriHOME EOx ceramides in human skin. Human epidermal breast tissue obtained from surgical donation was prepared and epidermal lipids extracted and analysed using LC/MS/MS as described in Methods. MS were extracted from the data in Figure 1A, with putative identification based on precursor *m/z* value, with product ion at *m/z* 329.2.

Supplemental Figure 12

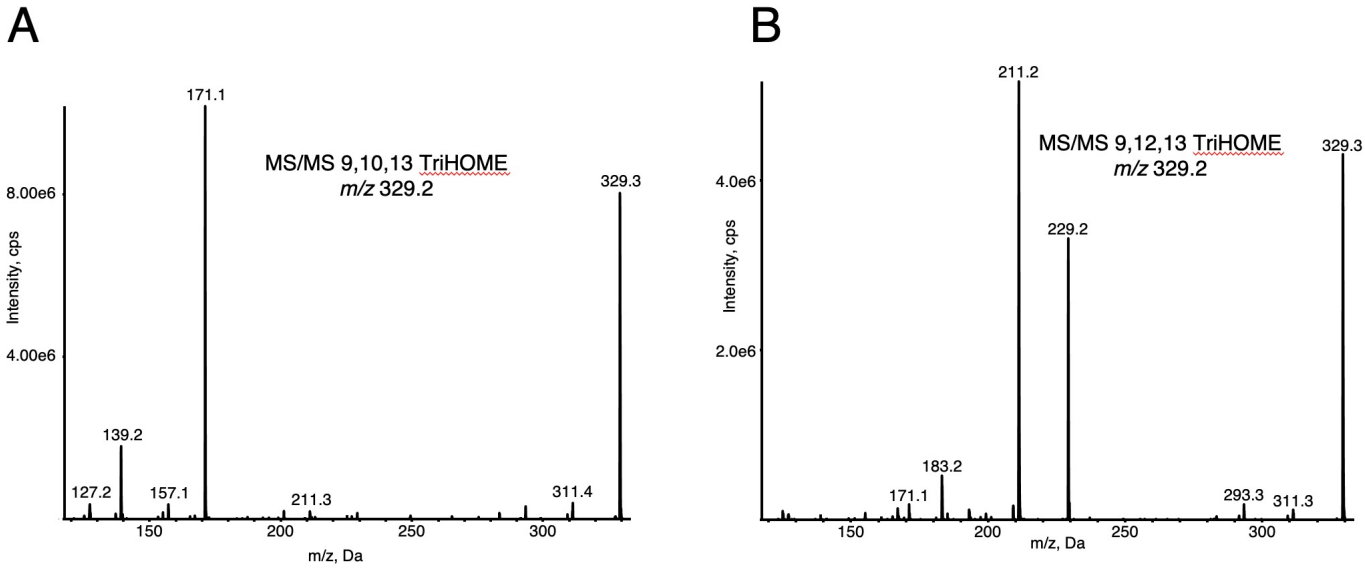

Supplemental Figure 12. MS/MS of two triHOME standards yielding expected product ions. Panel A – 0.5μg/ml 9*S*, 10*S*, 13*S* triHOME (Larodan Chemicals) was directly infused onto a ABSciex MS at 10μl/min with settings as follows: CUR 20, IS -4500V, GS1 12, GS2 0, CAD -3, DP -90V, EP -10V, CE -30V, TEM 0. Panel B – 0.5μg/ml 9*S*, 12*S*, 13*S* triHOME (Larodan Chemicals) was infused as above.

Supplemental Figure 13

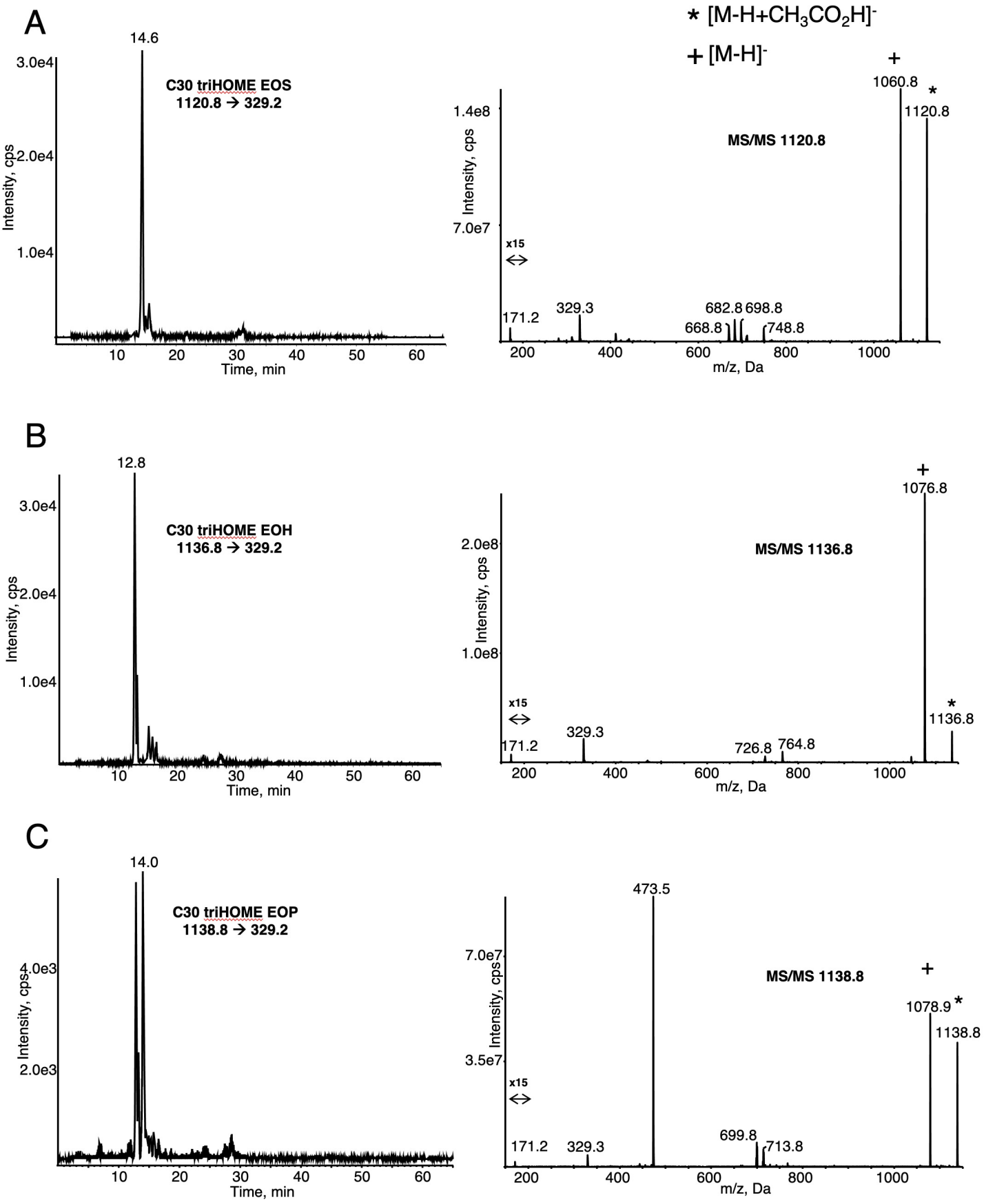

Supplemental Figure 13. MS/MS chromatograms and spectra for TriHome containing C30-EOx ceramides. Lipids extracted as in Supplemental Figure 11 were analysed using reverse phase LC/MS/MS as described in Methods, monitoring the precursor to product ion as shown in the left panels. Enhanced product ion (EPI) spectra were acquired in ion trap mode at the apex of elution for each lipid as described. Lipids were detected as $[M\text{-}H+CH_3CO_2H]^-$ ions.

Supplemental Figure 14

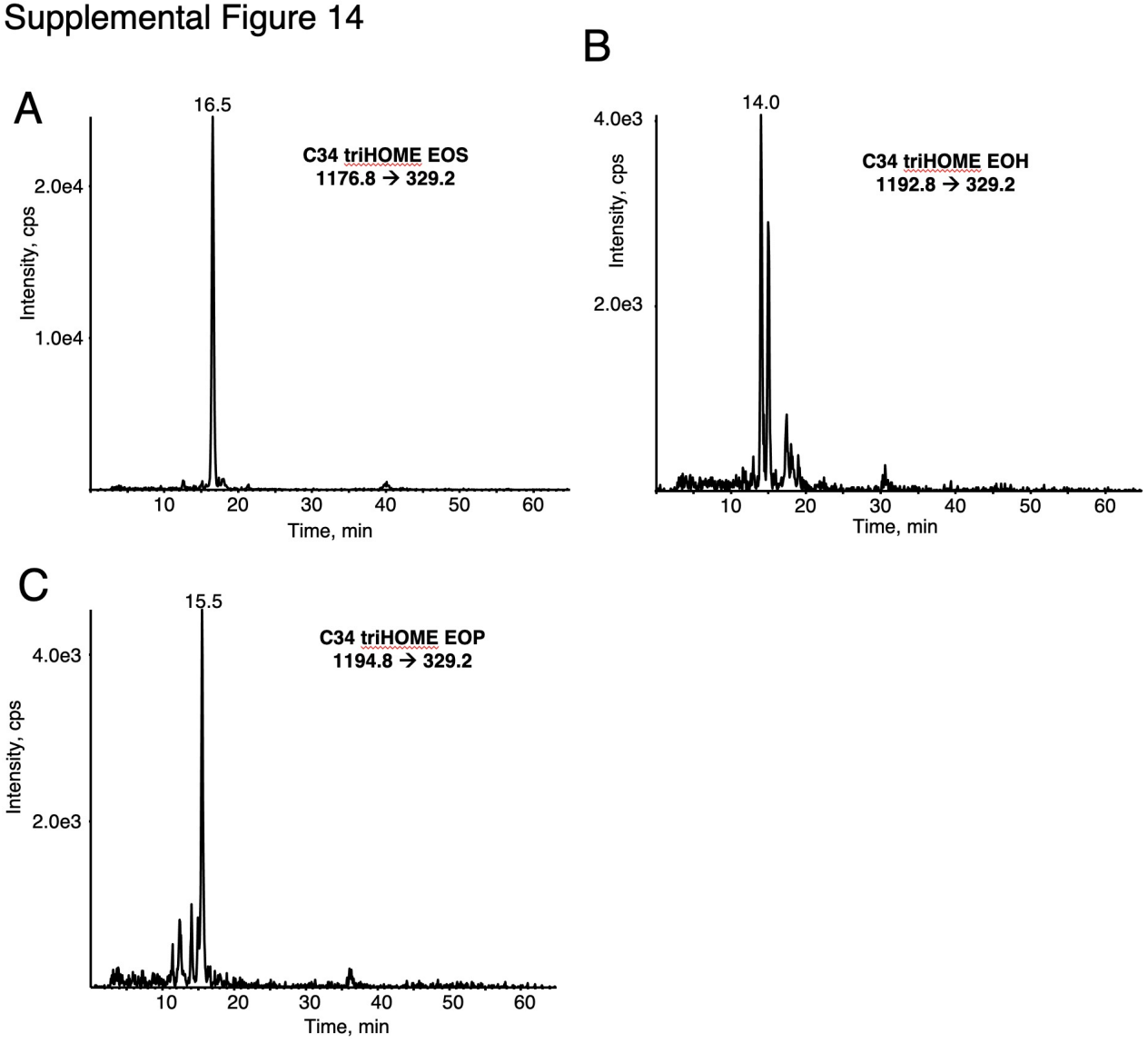

Supplemental Figure 14. MS/MS chromatograms and spectra for TriHOME containing C34-EOx ceramides. Lipids extracted as in Supplemental Figure 11 were analysed using reverse phase LC/MS/MS as described in Methods, monitoring the precursor to product ion as shown in the left panels.

Supplemental Figure 15

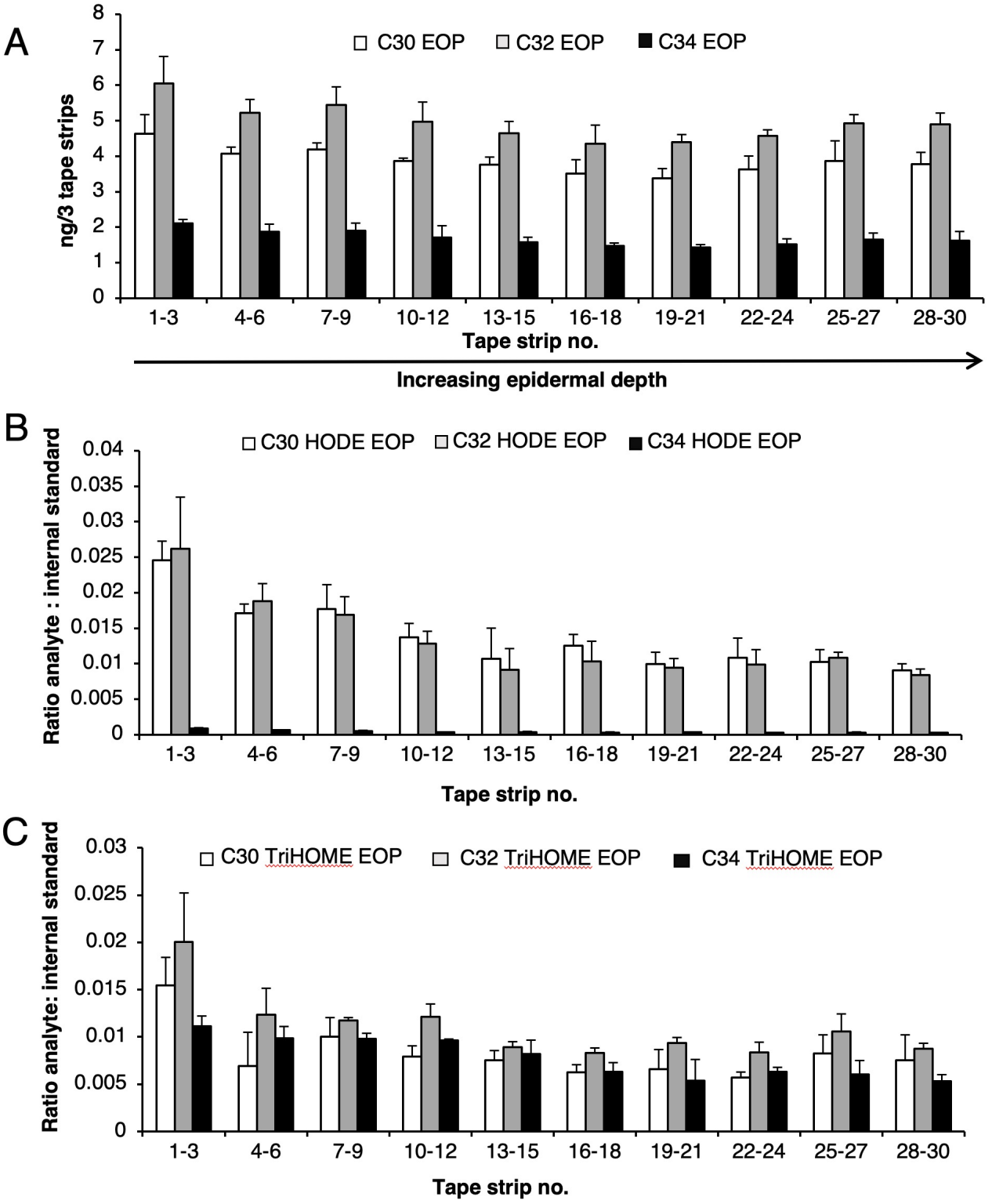

Supplemental Figure 15. Human epidermis shows higher levels of triHOME- and HODE-EOP in upper layers. Tape strips were acquired from the volar forearm of healthy volunteers (n=5 subjects, 30 strips per person, mean ± S.E.M). Strips were combined into groups of 3 and lipids extracted and analysed using LC/MS/MS as described in Methods for total levels of lipid present. *Panel A, LA-EOP is evenly distributed throughout the skin layers. Panels B,C. TriHOME EOP and HODE EOP are increased in the upper layers of epidermis and appear highest in the stratum corneum (SC).*

Supplemental Figure 16

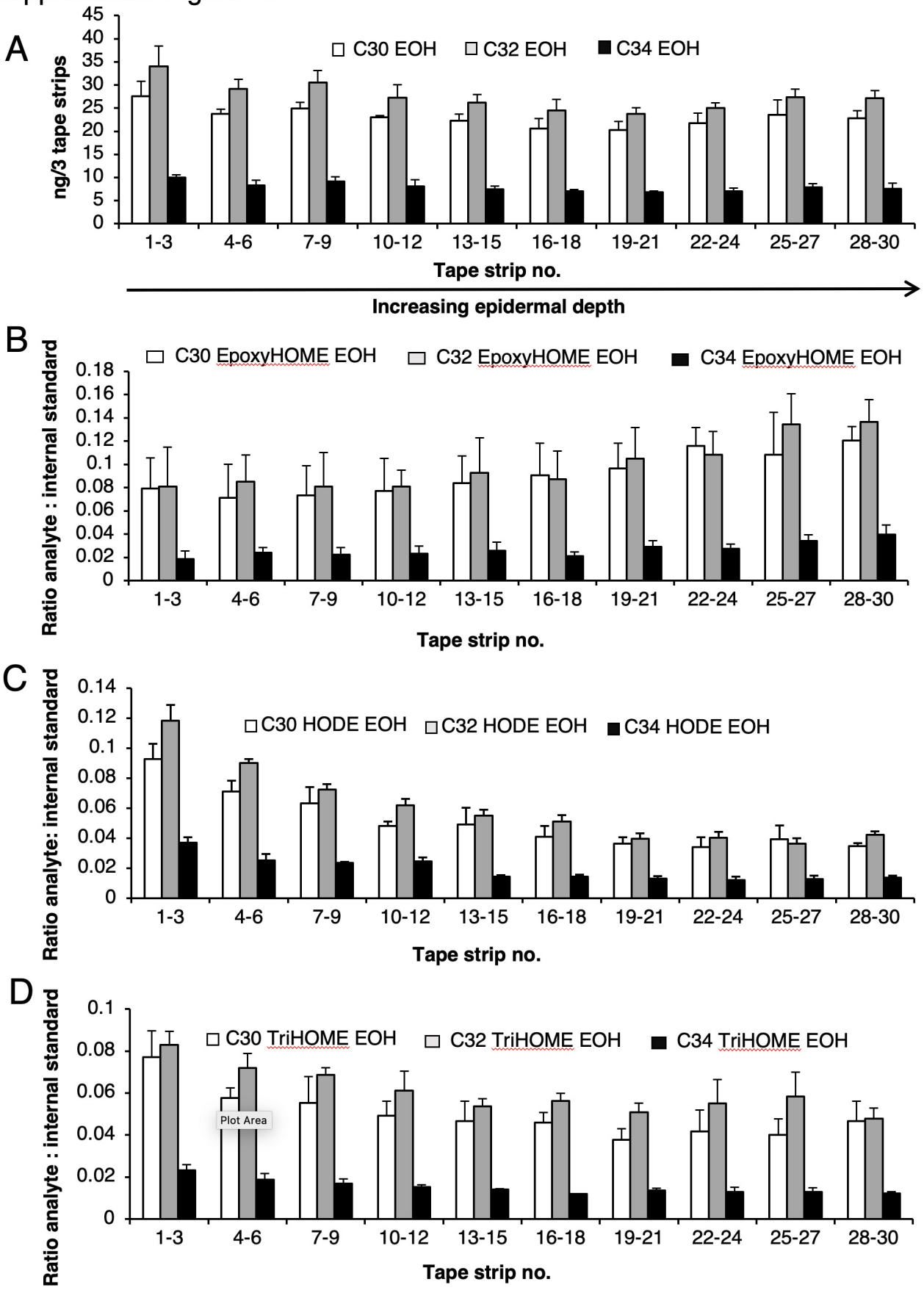

Supplemental Figure 16. Human epidermis shows higher levels of triHOME- and HODE-EOH, and reduced levels of epoxyHOME-EOH in upper layers. Tape strips were acquired from the volar forearm of healthy volunteers (n=5 subjects, 30 strips per person, mean ± S.E.M). Strips were combined into groups of 3 and lipids extracted and analysed using LC/MS/MS as described in Methods for total levels of lipid present. *Panel A, LA-EOH is evenly distributed throughout the skin layers. Panel B. Epoxy-HOME EOH increases with greater epidermal depth and is highest in the stratum granulosum/spinosum (SG, SS) layers. Panel C,D. TriHOME EOSHand HODE EOH are increased in the upper layers of epidermis and appear highest in the stratum corneum (SC).*

Supplemental Figure 17

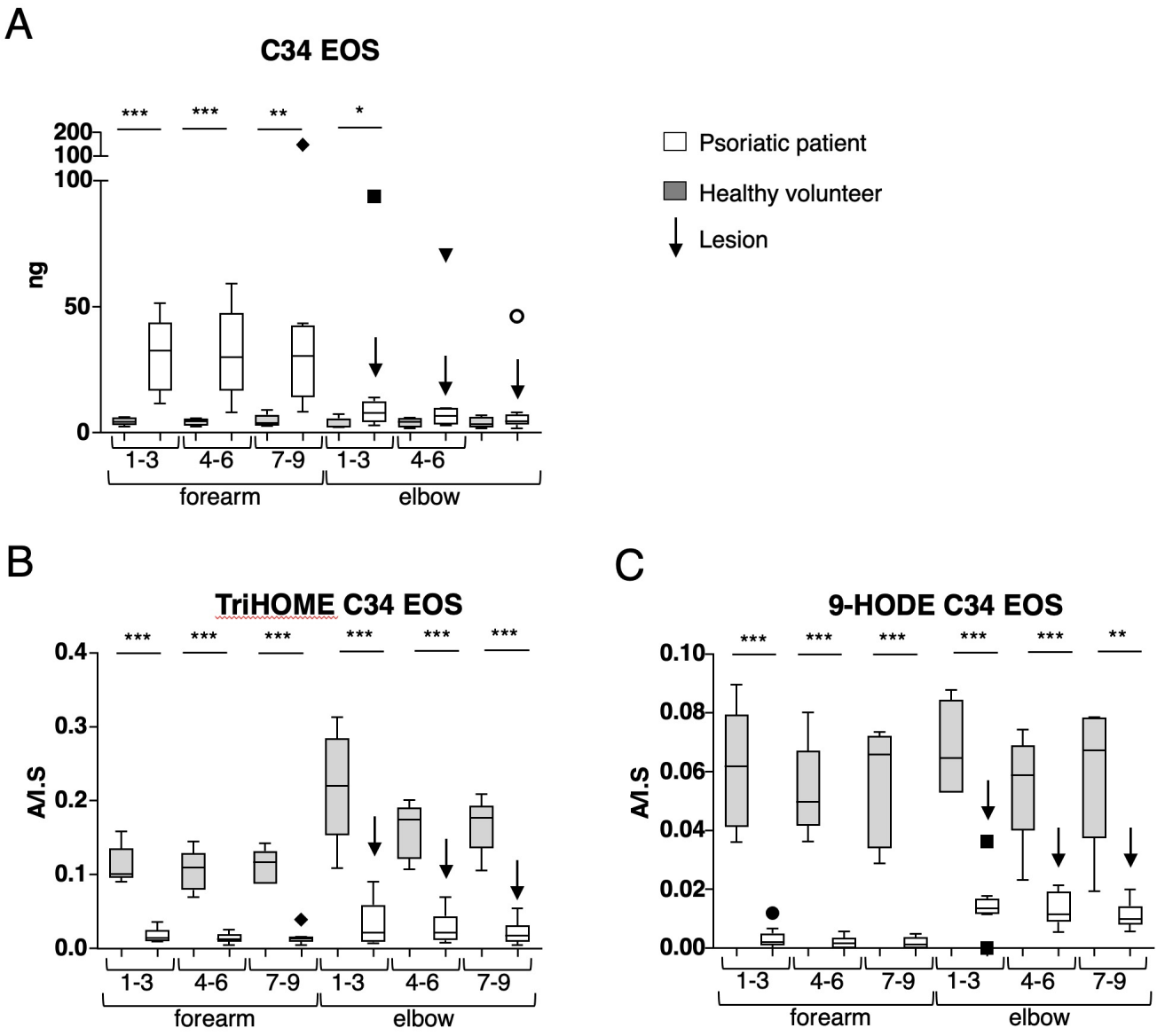

Supplemental Figure 17. Lipidomics analysis of psoriasis lesions shows elevated native EOx species, and significantly altered levels of oxidized species. Tape strips were acquired from the volar forearm (uninvolved skin) and elbow (location of psoriatic lesion), from patients with psoriasis (n = 9) and from healthy controls (n = 5). From each site, 9 tape strips were obtained and pooled into groups of 3. Lipids were extracted and analysed as described in Methods. Increasing tape strip number corresponds to increasing epidermal depth. Psoriatic patients (empty bars), healthy controls (grey bars), mean ± S.E.M.* = $p<0.05$, ** = $p<0.01$, *** = $p<0.001$. The bold down arrow (↓) corresponds to skin lesion samples. Geometric shapes show outliers. *Panel A, epidermal tape strip profile of C34 EOS. Panel B, epidermal tape strip profile of triHOME EOS. Panel C, epidermal tape strip profile of 9-HODE EOS in psoriatic vs healthy control.*

Supplemental Figure 18

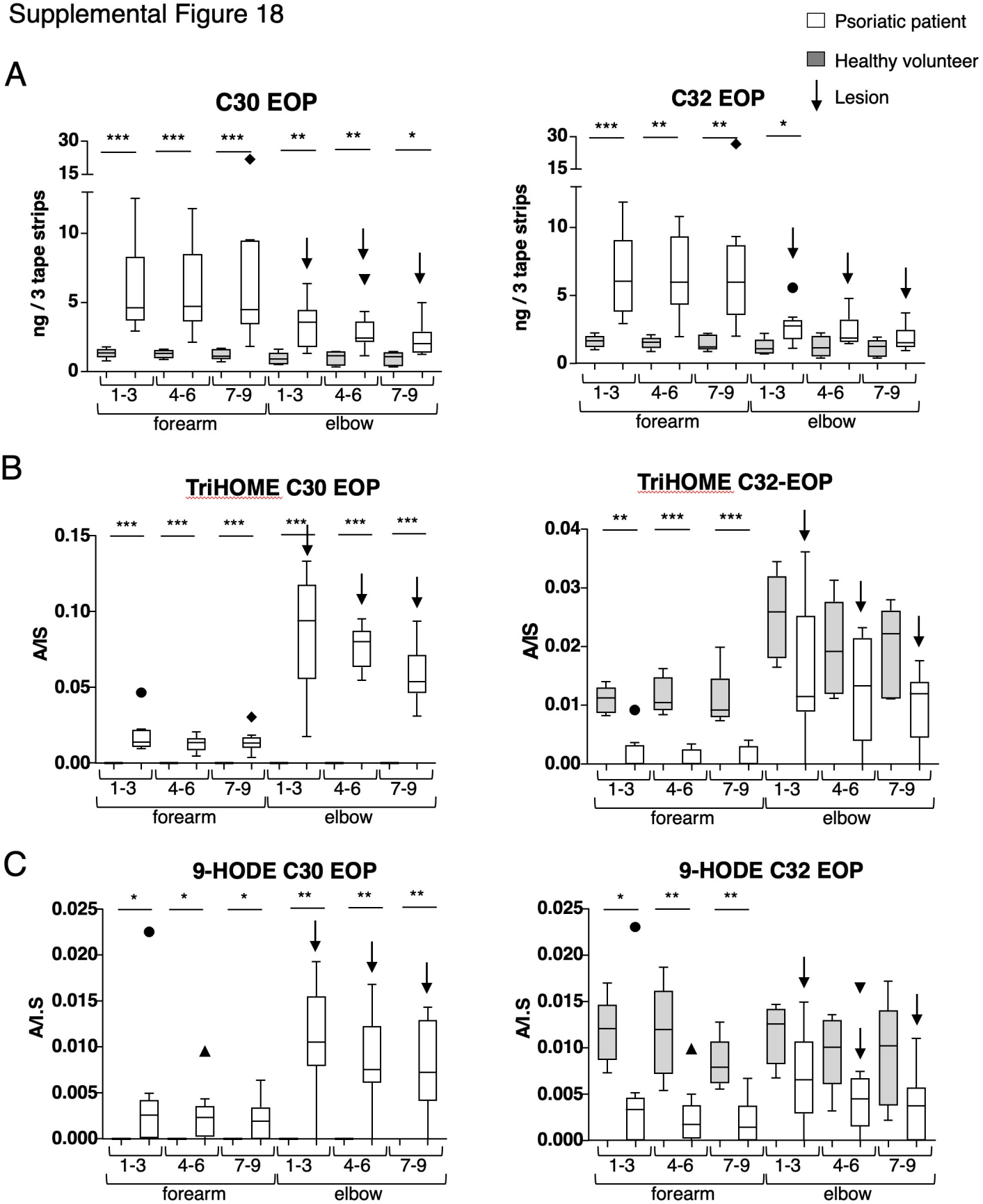

Supplemental Figure 18. Lipidomics analysis of psoriasis lesions shows elevated native EOx species, and significantly altered levels of oxidized species. Tape strips were acquired from the volar forearm (uninvolved skin) and elbow (location of psoriatic lesion), from patients with psoriasis (n = 9) and from healthy controls (n = 5). From each site, 9 tape strips were obtained and pooled into groups of 3. Lipids were extracted and analysed as described in Methods. Increasing tape strip number corresponds to increasing epidermal depth. Psoriatic patients (empty bars), healthy controls (grey bars), mean ± S.E.M.* = $p<0.05$, ** = $p<0.01$, *** = $p<0.001$. The bold down arrow (↓) corresponds to skin lesion samples. Geometric shapes show outliers. *Panel A, epidermal tape strip profile of C30 and C32 EOP. Panel B, epidermal tape strip profile of triHOME EOP. Panel C, epidermal tape strip profile of 9-HODE EOP in psoriatic vs healthy control.*

Supplemental Figure 19

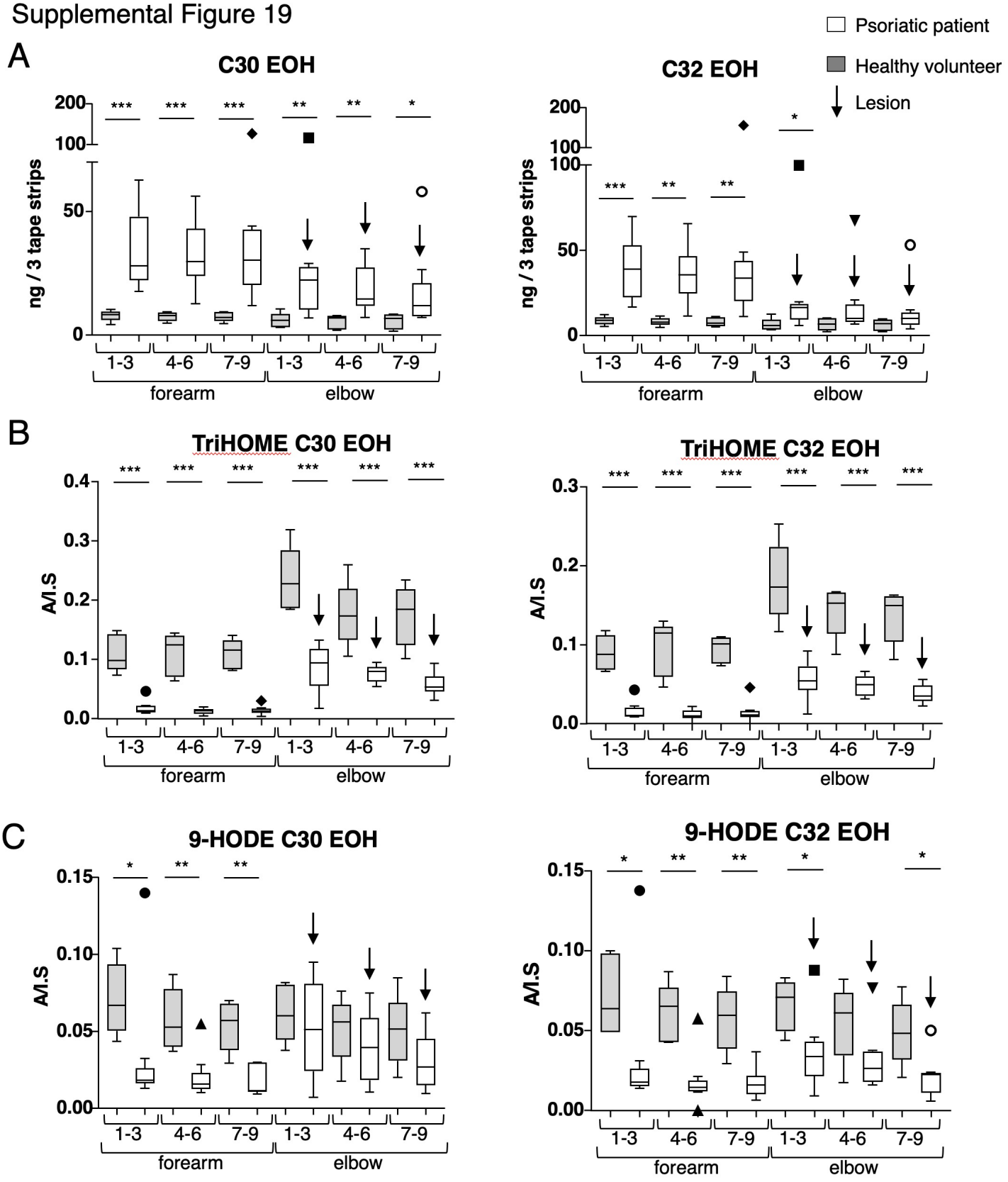

Supplemental Figure 19. Lipidomics analysis of psoriasis lesions shows elevated native EOx species, and significantly altered levels of oxidized species. Tape strips were acquired from the volar forearm (uninvolved skin) and elbow (location of psoriatic lesion), from patients with psoriasis (n = 9) and from healthy controls (n = 5). From each site, 9 tape strips were obtained and pooled into groups of 3. Lipids were extracted and analysed as described in Methods. Increasing tape strip number corresponds to increasing epidermal depth. Psoriatic patients (empty bars), healthy controls (grey bars), mean ± S.E.M.* = $p<0.05$, ** = $p<0.01$, *** = $p<0.001$. The bold down arrow (↓) corresponds to skin lesion samples. Geometric shapes show outliers. *Panel A, epidermal tape strip profile of C30 and C32 EOH. Panel B, epidermal tape strip profile of triHOME EOH. Panel C, epidermal tape strip profile of 9-HODE EOH in psoriatic vs healthy control.*

Supplemental Figure 20

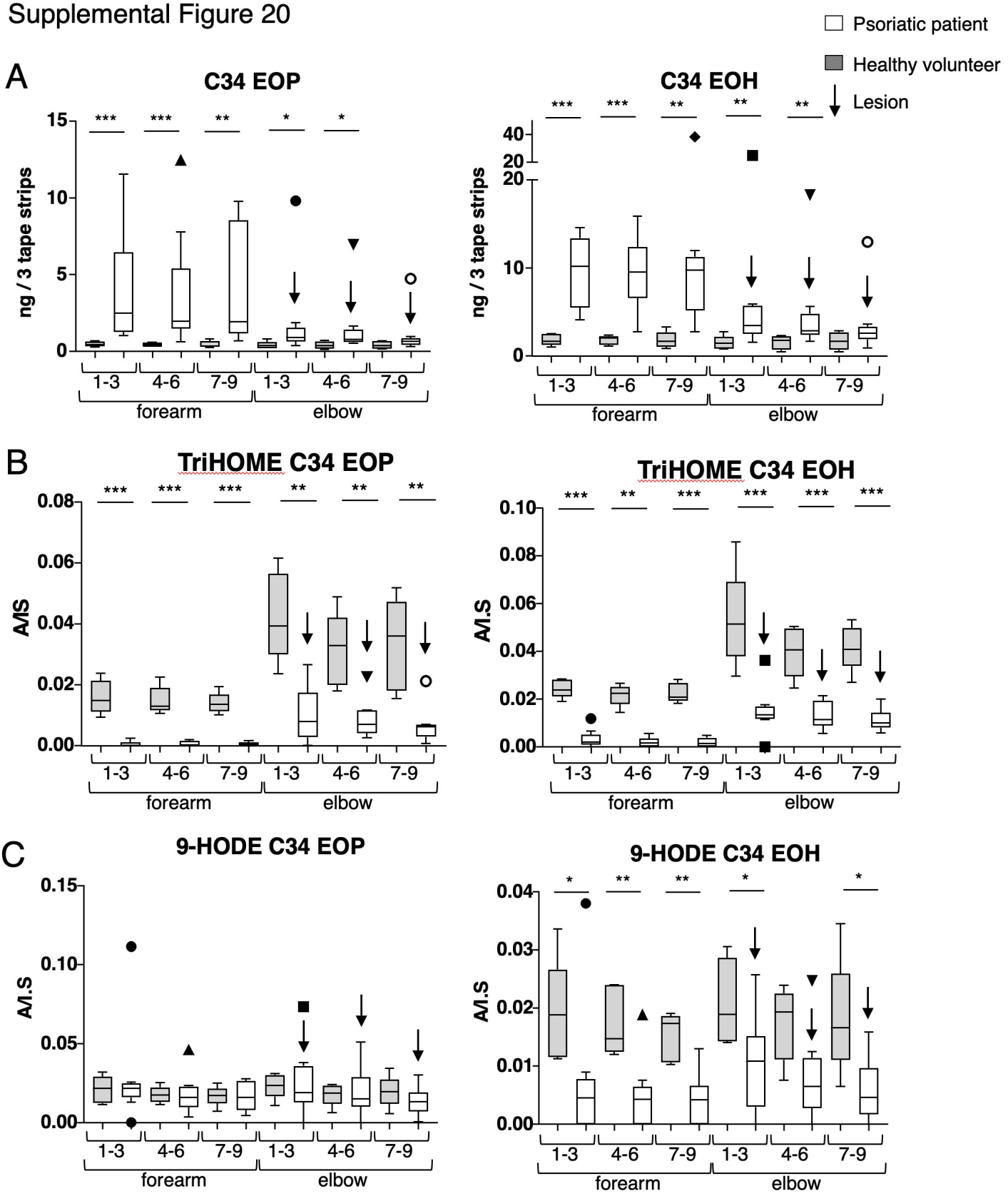

Supplemental Figure 20. Lipidomics analysis of psoriasis lesions shows elevated native EOx species, and significantly altered levels of oxidized species. Tape strips were acquired from the volar forearm (uninvolved skin) and elbow (location of psoriatic lesion), from patients with psoriasis (n = 9) and from healthy controls (n = 5). From each site, 9 tape strips were obtained and pooled into groups of 3. Lipids were extracted and analysed as described in Methods. Increasing tape strip number corresponds to increasing epidermal depth. Psoriatic patients (empty bars), healthy controls (grey bars), mean ± S.E.M.* = p<0.05, ** = p<0.01, *** = p<0.001. The bold down arrow (↓) corresponds to skin lesion samples. Geometric shapes show outliers. *Panel A, epidermal tape strip profile of C34 EOP and EOH. Panel B, epidermal tape strip profile of triHOME C34 EOP and EOH. Panel C, epidermal tape strip profile of 9-HODE C34 EOP and EOH in psoriatic vs healthy control.*